Chaos, Solitons and Fractals 142 (2021) 110424

Contents lists available at ScienceDirect

Chaos, Solitons and Fractals

Nonlinear Science, and Nonequilibrium and Complex Phenomena

journal homepage: www.elsevier.com/locate/chaos

Evolutionary dynamics in the rock-paper-scissors system by changing community paradigm with population flow

Junpyo Park

Department of Mathematical Sciences, Ulsan National Institute of Science and Technology, Ulsan 44919, Republic of Korea

ARTICLE INFO

Article history:
Received 15 June 2020
Revised 21 September 2020
Accepted 2 November 2020
Available online 21 November 2020

Keywords:
Rock-paper-scissors game
Population flow
Community paradigm
Multistability
Oscillatory behavior

ABSTRACT

Classic frameworks of rock-paper-scissors game have been assumed in a closed community that a density of each group is only affected by internal factors such as competition interplay among groups and reproduction itself. In real systems in ecological and social sciences, however, the survival and a change of a density of a group can be also affected by various external factors. One of common features in real population systems in ecological and social sciences is population flow that is characterized by population inflow and outflow in a group or a society, which has been usually overlooked in previous works on models of rock-paper-scissors game. In this paper, we suggest the rock-paper-scissors system by implementing population flow and investigate its effect on biodiversity. For two scenarios of either balanced or imbalanced population flow, we found that the population flow can strongly affect group diversity by exhibiting rich phenomena. In particular, while the balanced flow can only lead the persistent coexistence of all groups which accompanies a phase transition through supercritical Hopf bifurcation on different carrying simplices, the imbalanced flow strongly facilitates rich dynamics such as alternative stable survival states by exhibiting various group survival states and multistability of sole group survivals by showing not fully covered but spirally entangled basins of initial densities due to local stabilities of associated fixed points. In addition, we found that, the system can exhibit oscillatory dynamics for coexistence by relativistic interplay of population flows which can capture the robustness of the coexistence state. Applying population flow in the rock-paper-scissors system can ultimately change a community paradigm from closed to open one, and our foundation can eventually reveal that population flow can be also a significant factor on a group density which is independent to fundamental interactions among groups.

1. Introduction

For the fast decade, since applied to elucidate complex behaviors in real ecosystems [1–5], there have been greatly challenged on population systems of non-hierarchical cyclic competition in both macroscopic and microscopic levels. In general, from the perspective of survival states, biodiversity in cyclic competition systems have been interpreted based on a metaphor of rock-paper-scissors (RPS) game by exploiting additional interactions including noise [6], mobility [7–13], habitat suitability [14], intraspecific competition [15,16], mutation [17–22], quasi birth and death process [23], asymmetric niche and interactions [24–27], and interpatch migration [28,29] by presenting various nonlinear dynamical features [30–33]. In addition to implementing in ecosystems, rock-paper-scissors game has been exploited to understand dynamics in social sciences [34–37].

Typically, in classic approaches on RPS games, fundamental factors to affect a change of a density in each population group are interspecific competition (which is usually regarded by predation) and reproduction to lead the decrease and increase of a density, respectively, which imply that the change of population densities will depend on intracommunity interactions. Thus the entire structure of interactions among three groups is of a closed hypercycle. In real systems, however, in addition to such intracommunity interactions, a density of each group can be also affected by inflow and outflow of population, i.e., migration of population, which are commonly witnessed by various forms in ecological, biological, and social sciences [5,8,38–43]. For example, in market communities, those who want to start a business are willing to choose one of the promising businesses, and thus the start-up of a particular business may increase the size of the business itself. In the case of the establishment of the franchise industry, this process may increase the number of branches of the industry. However, an increase in the number of branches naturally causes

E-mail addresses: junpyopark80@gmail.com, jppark@unist.ac.kr

https://doi.org/10.1016/j.chaos.2020.110424
0960-0779/

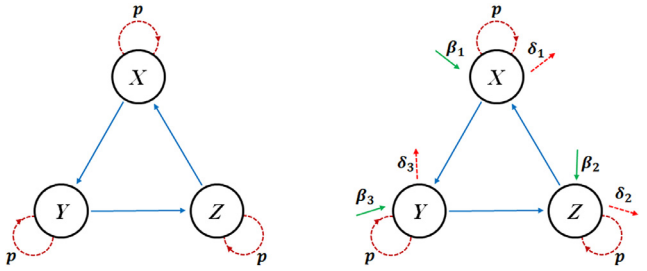

Fig. 1. Schematic diagrams of different community structures on rock-paper-scissors game: (a) a closed structure in classic systems and (b) an open structure with population flow. Blue straight arrows indicate intergroup competition which occurs with a rate 1 in a cyclic manner. In each group, red dashed loop demonstrates intragroup competition with a rate p, and green straight and red dashed arrows describe the inflow and outflow of populations in each group, respectively. (For interpretation of the references to colour in this figure legend, the reader is referred to the web version of this article.)

intergroup competition between branches, in which case sales may be stopped for branches with poor options. Besides, due to internal circumstances, it may happen that the store (or branches) will decide to shut down itself and the scale of such business markets may be getting smaller. Thus, in social sciences, such a flow process in groups or populations is a common feature and has a significant impact on the survival of each group. Nevertheless, even if there were several efforts to elucidate the effect of population flow on biodiversity of cyclic games within the framework of interpatch migration [28,29] which have been considered between finite patches, to the best of our knowledge, as an external factor to affect a density of a group in macroscopic levels, there is no attempt to address the population flow in rock-paper-scissors game.

Motivated from this point and in the perspective of changing community paradigm, in this paper, we investigate the effect of population flow on group diversity where the governing relationship among groups is the metaphor of rock-paper-scissors game. We describe population flow consisting of inflow and outflow in each group by implementing the mechanism of natural birth and death processes in classic Lotka-Volterra system [44,45], and develop an analytic theory based on the system of rate equations to explain numerical evidences and provide the effect of population flow. Briefly, our main findings are the followings. The first result is that, in contrast to previous works of rock-paper-scissors games under the closed community structure, balanced population flow can promote persistent coexistence by forming different carrying simplices which will depend on magnitudes of inflow and outflow. The second result is that imbalanced population can exhibit rich dynamics of group survivals by exhibiting alternative stable states consisting of various group survival states, emergence of multistability among single group survivals, and oscillatory dynamics for coexistence depending on relativistic interplay of flow magnitudes.

In Section 2, we model a rock-paper-scissors game with population flow in the macroscopic framework. In Section 3, we provide our results within two perspectives according to consideration of population flows numerically, and are analyzed mathematically in Section 4. Conclusion and discussions are addressed in Section 5.

2. Model

Fundamental reactions of rock-paper-scissors games adopting intragroup competition (see Fig. 1(a)) can be defined by the set of following rules [8,9,15,16,46,47]:

$$XY \xrightarrow{\sigma} X\varnothing, \quad YZ \xrightarrow{\sigma} Y\varnothing, \quad ZX \xrightarrow{\sigma} Z\varnothing, \tag{1}$$

$$X\varnothing \xrightarrow{\mu} XX, \quad Y\varnothing \xrightarrow{\mu} YY, \quad Z\varnothing \xrightarrow{\mu} ZZ, \tag{2}$$

$$XX \xrightarrow{p} X\varnothing, \quad YY \xrightarrow{p} Y\varnothing, \quad ZZ \xrightarrow{p} Z\varnothing, \tag{3}$$

where $\varnothing$ presents vacancies which can allow reproduction (2).

For well-mixed population, reactions (1)–(3) can be generally described by rate equations in the mean-field framework of May-Leonard limit. Let $x(t)$, $y(t)$, and $z(t)$ be the densities of three groups X, Y, and Z at time t, respectively. Then the deterministic system of three groups incorporating (1)–(3) can be written by the following set of rate equations [8,9,14,16,47]:

$$\begin{cases} \frac{dx(t)}{dt} = x(t)\left[\mu\{1-\rho(t)\} - \sigma z(t) - \frac{p}{2}x(t)\right], \\ \frac{dy(t)}{dt} = y(t)\left[\mu\{1-\rho(t)\} - \sigma x(t) - \frac{p}{2}y(t)\right], \\ \frac{dz(t)}{dt} = z(t)\left[\mu\{1-\rho(t)\} - \sigma y(t) - \frac{p}{2}z(t)\right], \end{cases} \tag{4}$$

where $\rho(t) = x(t) + y(t) + z(t)$ is the total density at time t.

In classic rock-paper-scissors models, changes of population densities can only occur either decreasing by intergroup competition (1) or increasing by reproduction (2), which means the density of each group ultimately depends on internal mechanisms. Thus, the entire structure of interplay can be regarded as "closed community" (see Fig. 1(a)). In real systems, however, the population density can be also affected by population inflow and outflow. For example, in cases of political parties, some nonaffiliated individuals may want to join one of political parties [48], or defected individuals may want to join another parties [33]. In this case, a density of certain group may increase by joining new members. In addition, members in a group may want to stop their political activities by intragroup competition or changing their political ideologies, and hence a group can become shrink by outflow of its members.

In this regard, considering population flow in each group may change the interplay structure as "open community" which is illustrated in Fig. 1(b), and we thus wonder how survivorship of competing groups can change by population flow. To address the effect of population flow on group diversity in the cyclic competition system, we simply implement a similar way to natural birth and death processes in the Lotka-Volterra system [44,45] to describe inflow and outflow of populations in each group, respectively. To make an unbiased comparison with previous works which has no population flow [8,9,16], we assume $\sigma = \mu = 1$. Then Eq. (4) can be rewritten by:

$$\begin{cases} \frac{dx}{dt} = x\left[(1-\rho) - z - \frac{p}{2}x + \beta_1 - \delta_1\right], \\ \frac{dy}{dt} = y\left[(1-\rho) - x - \frac{p}{2}y + \beta_2 - \delta_2\right], \\ \frac{dz}{dt} = z\left[(1-\rho) - y - \frac{p}{2}z + \beta_3 - \delta_3\right], \end{cases} \tag{5}$$

where β_i and δ_i $(i = 1, 2, 3)$ indicate the inflow and outflow rates of groups X, Y, and Z.

Such a description to inflow and outflow of populations by using several parameters may be eventually matched to the asymmetric rock-paper-scissors model [46], and may be regarded as natural birth and death in each group. Even if two terms for inflow and outflow in each group can be written by a single parameter, we will distinguish two parameters to realize and elucidate the effect of population flow in detail.

3. Results

In this section, we carry out numerical simulations to provide global aspects on the effect of population flow on biodiversity among three groups from two perspectives, which can be classified based on the symmetry of flows:

(a) *balanced population flow* that all groups have same inflow and outflow rates, i.e., $\beta_i = \beta$ and $\delta_i = \delta$ $(i = 1, 2, 3)$, where the two rates β and δ may be nonuniformly given, and

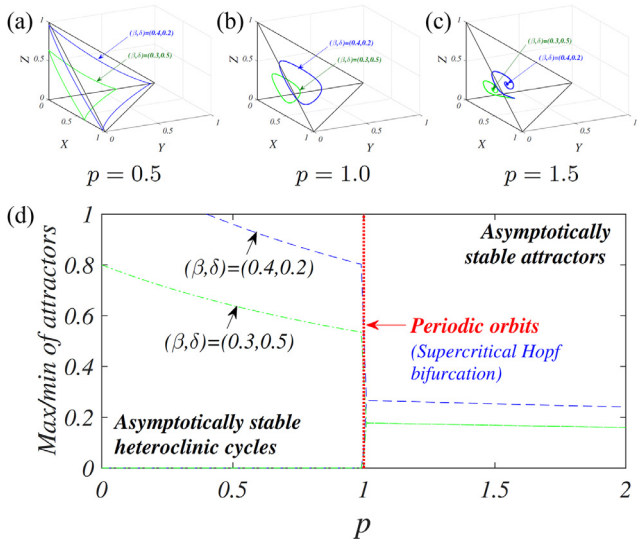

Fig. 2. (a–c) Phase transitions of attractors with different p and (d) maximum and minimum values of attractors of Eq. (5) depending on p. Parameters (β, δ) are given by $(0.4, 0.2)$ for tops and (0.3,0.5) for bottoms. The initial condition is given by (0.625,0.128,0.247). (a–d) As p increases, the system exhibits phases transitions from asymptotically stable heteroclinic cycles to periodic orbits, and asymptotically stable sinks which occurs on different carrying simplices. (d) The phase transition recasts in a wide spectrum of p through bifurcation diagram by measuring maximum and minimum values of attractors versus p. Regardless of (β, δ), Eq. (5) always exhibits the phase transition between heteroclinic cycles and sinks via $p = 1$.

(b) *imbalanced population flow* that all rates of inflow and outflow may be given nonuniformly which may indicate that both inflow and outflow rates may differ to each group.

We implement a Runge-Kutta method and symbolic calculations on our all numerical simulations to present phase portraits, basin structures, and certain probabilities.

3.1. Effect of balanced population flow: persistent coexistence with forming different carrying simplices

According to the analysis which will be explained in Section 4, we can predict that Eq. (5) may exhibit a phase transition between asymptotically stable heteroclinic cycles and asymptotically stable attractors constituted by an interior fixed point as the parameter p varies, where two states of heteroclinic cycles and attractors are noted by P_1 and P_3, respectively. To be concrete, regardless of choices of β and δ, such a phase transition only depends on p if parameters β and δ satisfy the common condition $\delta < \beta + 1$. Since the phase transition can occur whether p exceeds 1 or not, we consider p by 0.5, 1, and 1.5. In this regard, for given different parameters settings, e.g., $(\beta, \delta) = (0.4, 0.2)$ and (0.3,0.5) satisfying the condition $\delta < \beta + 1$, phase transitions and a bifurcation diagram with respect to the change of p are illustrated in Fig. 2.

As shown in Fig. 2(a–c), Eq. (5) exhibits a phase transition from heteroclinic cycles to sinks by showing periodic orbits as p increases. The interesting feature in phase portraits is the change of carrying simplices and invariant manifolds for solutions of the system. Previous works of rock-paper-scissors game with internal interplay have been depicted without changing the carrying simplex, and the formation of attractors started from simplex S_3 and is changed gradually by intragroup competition. By applying population flow, however, we found that the phases of solutions are formed on different carrying simplices, and the invariant manifold for attractors can be also affected. Such a phase transition of attractors in a wide spectrum of p are depicted concretely by utilizing a bifurcation diagram versus p as shown in Fig. 2(d), where a bifurcation diagram is derived by exploiting the maximum and

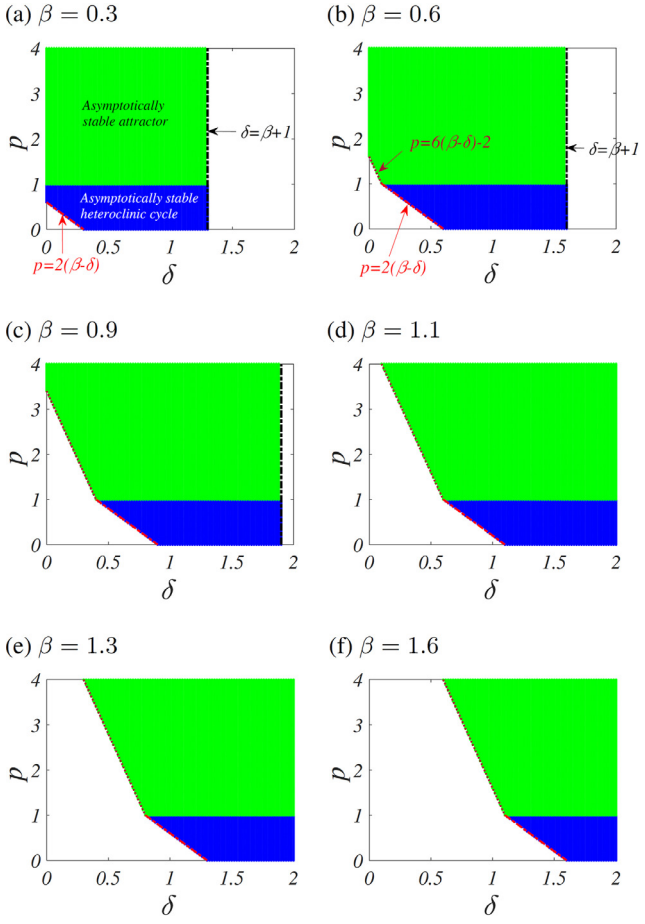

Fig. 3. Basins of asymptotically stable heteroclinic cycles(blue) and attractors(green) which are distinguished by $p = 1$ for all cases. The white region indicates that associated fixed points of P_1 and P_3 are not defined since the existence conditions of fixed points are not satisfied. As β increases, the basins move from left to right, and sufficiently high δ is required to validate stable existence of two states. (For interpretation of the references to colour in this figure legend, the reader is referred to the web version of this article.)

minimum value of the attractor in each p. In particular, similar to previous works [16,47,49], the phase transition can occur as Eq. (5) falls into the class of Hopf bifurcation in which is supercritical, and it is a common feature regardless of rates of population flow (β, δ) whenever the rates satisfy the condition $\delta < \beta + 1$ to validate existences of fixed points of P_1 and P_3, where two states are defined by (9)–(11) and (15) in Section 4.1, respectively. The stability of heteroclinic cycles featured in Fig. 2(a) can be determined by a calculation of the saddle value V which is defined by [50]:

$$V = \prod_{i=1}^{3} V_i = \left(\frac{2-p}{p}\right)^3 > 1, \quad {}^{\forall}p < 1 \tag{6}$$

for all fixed points (9)–(11) of P_1, and we easily find that the rate of intragroup competition p is the only parameter to determine the stability of heteroclinic cycles (see Theorem 1 in Section 4.1). Thus, as illustrated in Fig. 2, controlling p as a bifurcation point can yield a common phase transition regardless of (β, δ): from heteroclinic cycles to attractors in which are asymptotically stable accompanying with periodic orbits.

In addition, from Fig. 2(d), we find that the stable coexistence can be sensitively affected by both population flow and intragroup competition. For example, for $(\beta, \delta) = (0.4, 0.2)$, the solution can be validated for $p > 0.4$ while that with $(\beta, \delta) = (0.3, 0.5)$ is defined for $p \geq 0$. In other words, Eq. (5) may not have any fixed

points depending on the choice of (β, δ) with respect to p, which may imply that there may be a phase transition of basins of parameters for stable fixed points of P_1 and P_3. To be concrete, such phase transitions of basins of parameters consisting of (δ, p) by fixing β for instance are presented in Fig. 3 where borders among distinct basins indicate the thresholds of existence and stability conditions of corresponding fixed points of P_1 and P_3.

From Fig. 3, we found that, for the considered range of δ, the higher inflow rate requires a relatively high outflow rate for validating P_1 and P_3 which are indicated by blue and green colors. For white regions in each panel in Fig. 3, we have no particular indications of associated dynamical behaviors. In the white regions, fixed points of P_1 and P_3 are not defined, i.e., the existence conditions of fixed points of two states are not satisfied. In this case, when we consider parameters in the white regions, the system may exhibit two features either (i) the trajectories of solutions of the system will converge to the origin where the interior fixed point of P_3 has negative components; or (ii) the total density of three groups exceeds 1 even if the density of each group is less than 1.

Under balanced population flow, we found that the interplay between inflow and outflow of the population which is affected by intraspecific competition can lead to stable coexistence. While the asymptotically stable heteroclinic cycle which is constituted by three absorbing fixed points of P_1 can be appeared by the extinction state on spatially extended systems [8,14,16,32], it may indicate a weak coexistence because solutions of Eq. (5) are eventually traveling near the cycle. Nevertheless, it is obvious that the balanced flow can facilitate persistent coexistence of all groups.

3.2. Rich dynamics by imbalanced population flows

3.2.1. Basin structures of parameters of imbalanced flow for diverse survival states

We now explore dynamical features with imbalanced population flow. In a similar approach to the balanced flow, we can obtain that the Eq. (5) with imbalanced (nonuniform) population flows can also possess three types of survival states, Q_1, Q_2, and Q_3 for describing survival of only one group, existences of two interacting groups, and coexistence of all groups, respectively, which are defined by the number of surviving groups (see the detailed form of associated fixed points in Appendix A).

Since there are several unknown parameters to be considered, unfortunately, it is quite difficult to gain overall dynamical features simultaneously. To handle this issue, we may imagine the following situation: For example in social sciences, in a particular business situation, when competition among groups in similar fields is active and each group is growing well, the influx of new participants to join (or invest) each group can sometimes overheat while the outflow may differ from group to group by characteristics [51–54]. In this case, it is possible to restrict excessive inflow into groups overall. Based on such a plausible situation, we may assume that the inflow rates in all groups may be restricted within a certain level, which means the total amount of inflow rates may be given by a constant: $\sum_{i=1}^{3} \beta_i = \Lambda$, where the initial outflow rate in each group is given nonuniformly. In this pursuit, based on the linear stability analysis of fixed points of three distinct survival states Q_1, Q_2, and Q_3, the overall dynamics of group diversity by population inflow can be presented on a triangular phase space of inflow rates which are illustrated in Fig. 4.

Fig. 4 shows the basin structure for each stable state in Eq. (5) for the given nonuniform outflow rates $(\delta_1, \delta_2, \delta_3) = (0.1, 0.3, 0.4)$. According to the combination of β_i $(i = 1, 2, 3)$, Eq. (5) exhibits various dynamical features on survival states which are defined by the number of surviving groups while the balanced population flow can only lead to persistent coexistence. In particular, the imbalanced population flow can yield survival states of any two interacting groups on cyclic dominant relationships which are not observed in the balanced population flow in Section 3.1. In this case, we found that (a) the basin structure on the phase space does not present all states of Q_2, and (b) any one of survival states can only appear at moderate rates of inflows and intragroup competition, which may imply that the survival states will be sensitively

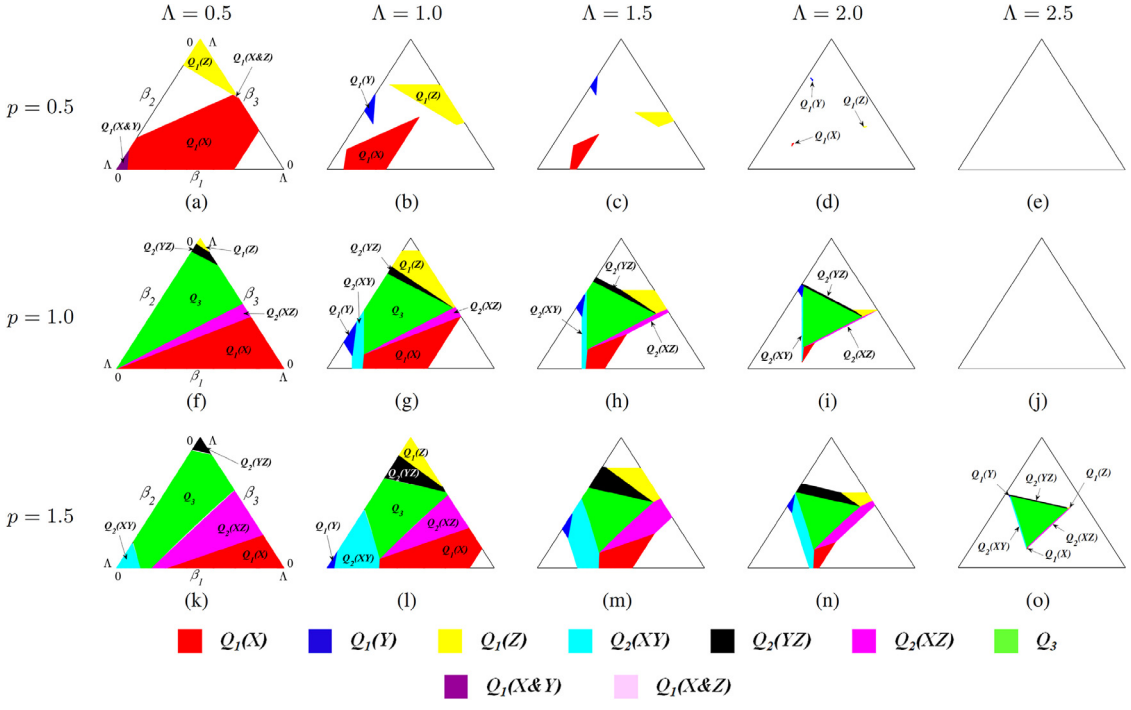

Fig. 4. Basin structures for nonuniform inflow rates with fixed nonuniform outflow rates $(\delta_1, \delta_2, \delta_3) = (0.1, 0.3, 0.4)$. In each panel, colors indicate basins of parameters for different survival states. According to the symmetry-breaking of inflow rates, Eq. (5) can possess various survival states which can be well-defined by both p and Λ, and exhibit multistable states as shown in (a). On the other hand, if the total population inflow exceeds a certain level, the system does not show any survival state.

determined by the combination of interaction rates. In each given p, the almost of inflow rates of a small amount of Λ may validate the existence of one of the survival states. As Λ increases, however, the portion of basins for stable survival states are decreasing and certain values of Λ relatively larger than p do not yield any type of basin structures as shown in Fig. 4(e) and (j). The reason why stable survival states are decreasing with the increase of Λ may be predicted by linear stability analysis of corresponding fixed points and sensitive interplay between intergroup and intragroup competition. Thus, specific types of fixed points can be defined for the given parameter setting on outflows.

It has been generally accepted that moderate or strong intragroup competition can promote coexistence of cyclic competing three groups [16,32,47,49] which associates to Q_3 in our model. However, even if for $p = 1$, Fig. 4 shows that no survival state including Q_3 is defined. To be concrete, for the large amount of inflow rates such as $\Lambda = 2.5$, the system does not present any survival state on the phase space of parameters for $p = 1$. On the contrary, for $p = 1.5$ which is shown in Fig. 4(o), the level $\Lambda = 2.5$ still exhibit basins of states Q_1, Q_2, and Q_3, even if basins of Q_1 and Q_2 are very small. Based on the basin structure, we may find that the strength of intragroup competition can increase as the total level of inflows increases, and address that the viability of groups can be sensitively affected by both population flow and intragroup competition.

3.2.2. Emergence of multistability among sole survival states

Even if basins are quite narrow, the feature to focus on the basin structure in Fig. 4 is the emergence of multistability. To be concrete, Fig. 4(a) exhibits two basins of parameters to lead multistable states between two fixed points in Q_1: $Q_1(X\&Y)$ and $Q_1(X\&Z)$. From the phase transition of basin structures as Λ increases, we may expect that the lower Λ may also yield multistabilities among fixed points of Q_1. Since it is still ambiguous of the multistability of different types of fixed points, to investigate the emergence of multistability in detail by considering cases constituted by fixed points of different classes for the given parameter for outflow, we measure the probability P_M that how multistability state can arise frequently depending on the flow mechanism, where P_M is defined by [33,47,49,55]:

$$P_M = \frac{n\{(\beta_1,\beta_2,\beta_3) \mid \exists \text{ multistable among } Q_i (i=1,2,3)\}}{n\left\{(\beta_1,\beta_2,\beta_3) \;\middle|\; \sum_{i=1}^{3}\beta_i = \Lambda,\ {}^{\forall}\beta_i \geq 0\right\}}, \quad (7)$$

and the P_M exhibits that the multistability can only emerge between any two fixed points of Q_1 for specific ranges of Λ and p as presented in Fig. 5(a)–(c). In our model, there is no possibility to observe the multistable states of all fixed points of Q_1 as shown in Fig. 5(d).

For the given outflow rates, we find that, specific cases of multistable states between two states in Q_1, in particular $Q_1(X\&Y)$ and $Q_1(X\&Z)$, can be revealed more frequently. In particular, for two states $Q_1(X\&Y)$ and $Q_1(X\&Z)$, phase portraits of solutions and corresponding basin structures of initial conditions under specific parameter settings are presented in Fig. 6.

The emergence of multistability among sole group survivals in systems of evolutionary dynamics has been already reported in Refs. [31,33], where the interplays in the proposed systems are slightly changed either bidirectional competition or transferring individuals among groups. The interesting feature on multistability in our model is the formation of basins of initial conditions for multistable states. While the phase space of initial conditions has been fully covered by any one of basins for sole states when the multistability of extinction occurs in previous works, we observe that, according to the multistable state, basin structures can be discontinuous depending on inflow rates. To be concrete, for the given setting of inflow rates, as depicted in Fig. 6(b), two basins of initial conditions for $Q_1(X)$ and $Q_1(Z)$ are spirally entangled and do not cover the phase space S_3 entirely while those for $Q_1(X)$ and $Q_1(Y)$ fully cover the phase space S_3 and are distinguished into two regions as shown in Fig. 6(a). Thus, we can conclude that multistability emerges among the sole group survivals and is more sensitive to the initial densities of the three groups under population flow, especially at low levels of inflow.

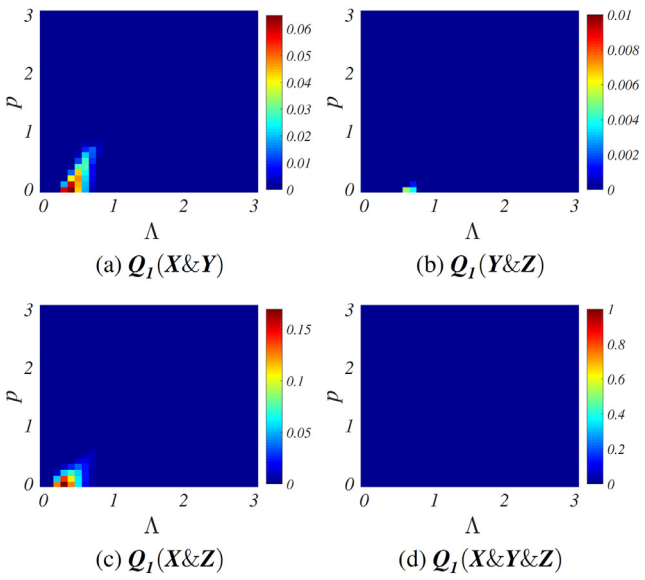

Fig. 5. Degree of multistability P_M among fixed points of Q_1 in combination with Λ and p. In the given outflow rates, when the strength of intragroup competition is quite weak, Eq. (5) can exhibit multistable states of any two points in Q_1 with respect to inflow rates at small ranges, i.e., an inflow rate β_i of each group is quite small.

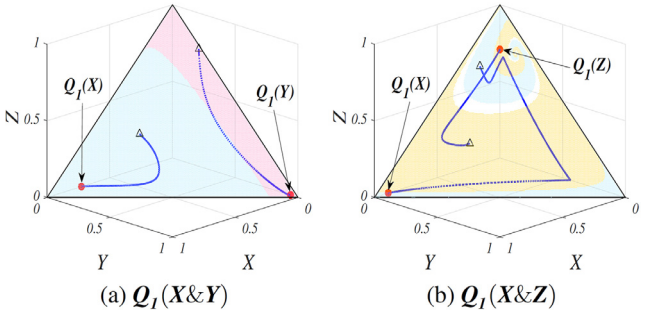

Fig. 6. Phase portraits and corresponding basins of initial conditions for the multistability in Q_1 with $(\Lambda, p) = (0.5, 0.5)$ associated to Fig. 4(a). In each figure, a triangle and a bullet indicate the initial condition and one of fixed point of Q_1, respectively. Basins of initial conditions for corresponding fixed points are presented by different colors. (a) For parameters $(\beta_1,\beta_2,\beta_3) = (0.0055, 0.476, 0.0185)$ satisfying $\Lambda = 0.5$, solutions of Eq. (5) starting from different initial conditions can converge to one of fixed points either $Q_1(X)$ or $Q_1(Y)$. (b) Similar to (a), the system exhibits multistable states of $Q_1(X)$ and $Q_1(Z)$ depending on the initial condition where the parameter set of inflow rates is given by $(\beta_1,\beta_2,\beta_3) = (0.214, 0.003, 0.283)$.

3.2.3. Characterizing robustness of coexistence by interplay between flow and intragroup competition

Even if the effect of imbalanced flow is explored through Fig. 4, understanding balance of flows according to intragroup competition is still ambiguous since Q_3 can be stable sensitively depending on both flows and intragroup competition as shown in Fig. 4. To be concrete, when a rate of intragroup competition p is fixed which is sufficiently large to yield stable coexistence, the basin of parameters $(\beta_1,\beta_2,\beta_3)$ for coexistence is shrinking and may dis-

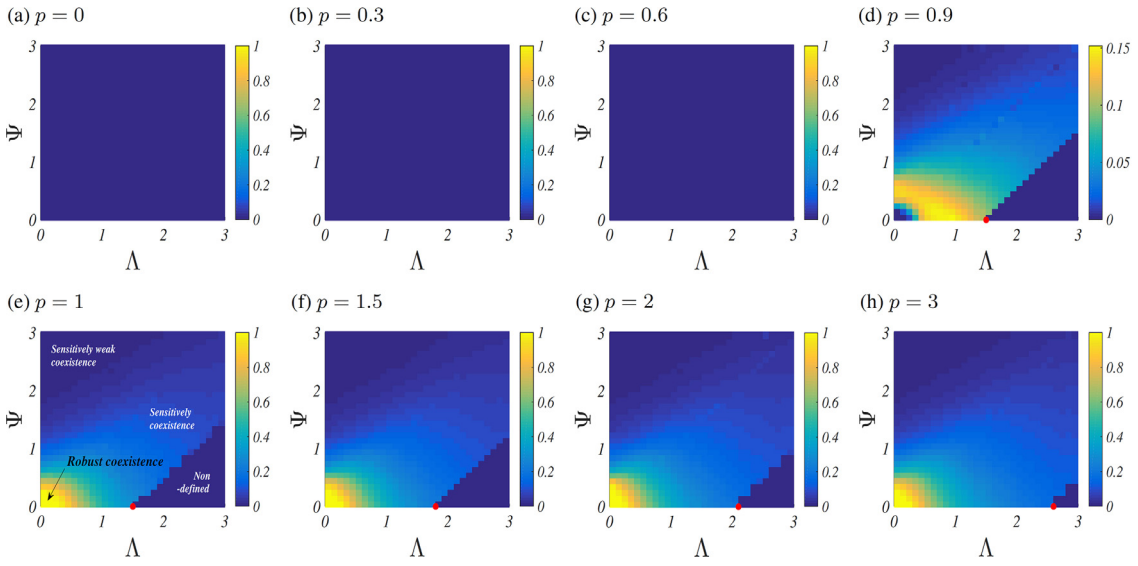

Fig. 7. The probability S_{coex} (8) in a combination with Λ and Ψ for different p. (a-c) For lower p associated to weak intragroup competition, there is no parameter combinations of population flow to yield stable coexistence. (d) As p increases, population flow can affect coexistence even if small amounts of sets are constituted. (e-h) For $p \geq 1$, the flow can strongly lead stable coexistence with weak levels of Λ and Ψ. Each panel may be classified by four regions of parameters with respect to the sensitivity of coexistence on population flow. In each panel, the red bullet indicates the threshold of Λ that Q_3 is not defined which also increases as p increases. (For interpretation of the references to colour in this figure legend, the reader is referred to the web version of this article.)

appear as the amount of Λ increases. In this regard, to predict the stable coexistence and characterization of the robustness of coexistence when it occurs stably, it is necessary to explore the interplay between population flow and intragroup competition. Characterizing the interplay and robustness may be evaluated by the number of components of all rates for stable coexistence, referred to as *the sensitivity of coexistence* S_{coex}, which can imply the degree of coexistence based on the basin area. To implement the sensitivity, we assume that both inflow and outflow can vary at certain levels: $\sum_{i=1}^{3}\beta_i = \Lambda$ and $\sum_{i=1}^{3}\delta_i = \Psi$, respectively. In this regard, similarly to P_M (7), the sensitivity of coexistence can be calculated by [31,33,47,49,55]:

$$S_{coex} = \frac{n\{(\beta_1,\beta_2,\beta_3,\delta_1,\delta_2,\delta_3) \mid \exists \text{ stable coexistence}\}}{n\left\{(\beta_1,\beta_2,\beta_3,\delta_1,\delta_2,\delta_3) \;\middle|\; \sum_{i=1}^{3}\beta_i = \Lambda,\ \sum_{i=1}^{3}\delta_i = \Psi,\ {}^{\forall}\beta_i,\delta_i \geq 0.\right\}}, \quad (8)$$

where Λ and Ψ range on $0 \leq \Lambda, \Psi \leq 3$ for the given $p \geq 0$, and the landscapes of S_{coex} with different p are illustrated in Fig. 7.

From the landscape of S_{coex} in Fig. 7, we found that stable coexistence is sensitively affected by population flow and intragroup competition. In particular, the classification of robustness of stable coexistence can be captured by oscillatory dynamics of solutions depending on total magnitudes of inflow and outflow which has been also featured in other frameworks of mathematical models [56,57]. For the weak intragroup competition, as shown in Fig. 7(a)–(c), there is no attempt that all groups can coexist for any frequency of population flow. The stable coexistence, i.e., the Q_3 becomes a stable attractor, can be possible as p increases even if small amounts of parameter sets can validate which are detected by low probability as in Fig. 7(d). As illustrated in Fig. 7(e)–(h), such stable behavior can similarly appear as p increases, and small levels of λ and Ψ in each p with $p \geq 1$ can yield the robust coexistence which corresponds to $S_{coex} = 1$. The interesting point is the transition of a critical Λ (which is indicated by the red bullet) that the degree S_{coex} becomes 0. To be concrete, for $p \geq 1$, the critical point increases at the same time as p increases. Even if a small area of parameters of Λ and Ψ can validate Q_3, the coexistence can appear sensitively depending on imbalanced flows with low probabilities overall as intragroup competition is intensified.

Intrinsically, if population outflows are more frequent than inflows, all groups will not be able to coexist, and we found that, by S_{coex}, the phenomenon occurs even if intragroup competition is moderate or strong. The landscape of S_{coex} provide that coexistence can be sensitively affected by population flow considering intragroup competition, and in particular, strong (robust) coexistence can be only promoted for the weak level of inflow and outflow overall.

In the absence of population flow either balanced or imbalanced, the system which can be defined by (4) can only exhibit three distinct phases without showing multistabilities among distinct survival states, and the overall feature are similarly obtained to the case of balanced flow. However, the survival states of three groups can be strongly changed under imbalanced flow of populations by exhibiting various survival states, multistability among single group survivals, and oscillatory behaviors for coexistence depending on relativistic relations between flow magnitudes.

4. Analysis

We now provide theories based on linear stability analysis to support our numerical findings. Within two perspectives of population flow either balanced or imbalanced case, the linear stability analysis for fixed points are similarly obtained for all cases. Thus, we provide the analysis in detail for the case of balanced population flow, and focus on the emergence of multistability and survival of two interacting groups for imbalanced flow.

4.1. Balanced population flow

Under the uniform consideration of each inflow and outflow rate to yield balanced flow, direct calculations $dx/dt = dy/dt = dz/dt = 0$ can yield that Eq. (5) can possess three distinct survival states which can be classified by the number of surviving groups.

Proposition 1. *Under the condition* $\beta + 1 > \delta$ *with* $\beta, \delta > 0$, *Eq. (5) possesses three types of fixed points which can be defined with additional conditions:*

(a) *P_1 for the survival of only one group:*

$$\left(\frac{2(\beta-\delta+1)}{p+2},0,0\right), \tag{9}$$

$$\left(0,\frac{2(\beta-\delta+1)}{p+2},0\right), \tag{10}$$

$$\left(0,0,\frac{2(\beta-\delta+1)}{p+2}\right), \tag{11}$$

for $2(\beta-\delta)\le p$,

(b) *P_2 for survivals of any two interacting groups:*

$$(\tilde{x},\tilde{y},0)=\left(\frac{2p(\beta-\delta+1)}{p^2+4p-4},\frac{2(p-2)(\beta-\delta+1)}{p^2+4p-4},0\right), \tag{12}$$

$$(0,\tilde{y},\tilde{z})=\left(0,\frac{2p(\beta-\delta+1)}{p^2+4p-4},\frac{2(p-2)(\beta-\delta+1)}{p^2+4p-4}\right), \tag{13}$$

$$(\tilde{x},0,\tilde{z})=\left(\frac{2(p-2)(\beta-\delta+1)}{p^2+4p-4},0,\frac{2p(\beta-\delta+1)}{p^2+4p-4}\right), \tag{14}$$

which are defined by $p>2$, *and*

(c) *P_3 for coexistence of all groups:*

$$(x^*,y^*,z^*)=\frac{2(\beta-\delta+1)}{p+8}(1,1,1), \tag{15}$$

for $6(\beta-\delta)-2\le p$.

Proof. Since we easily obtain fixed points of forms above by direct calculations, we here only prove the existence condition of each fixed point.

We first investigate the stability of fixed points (9)–(11). According to the form of the fixed points, we may easily find the existence condition which satisfies the followings:

$$\begin{aligned}&0\le\frac{2(\beta-\delta+1)}{p+2}\le 1\\ \Rightarrow\ &2(\beta-\delta+1)\le p+2\\ \Rightarrow\ &2(\beta-\delta)\le p,\end{aligned}$$

where the border defined by $p=2(\beta-\delta)$.

For the fixed points (12)–(14) of P_2, the components among three points are circulant, and thus, due to the symmetry, we investigate the stability of P_2 by employing the fixed point (12):

$$(\tilde{x},\tilde{y},0)=\left(\frac{2p(\beta-\delta+1)}{p^2+4p-4},\frac{2(p-2)(\beta-\delta+1)}{p^2+4p-4},0\right).$$

For $p\in\mathbb{R}_+$, the sign of denominator p^2+4p-4 changes either negative for $0<p<-2+2\sqrt{2}$ or positive for $p>-2+2\sqrt{2}$. For the parameter p on $0<p<-2+2\sqrt{2}$, since the value $\tilde{x}$ should be positive, we obtain the condition $p>0$ and $\beta-\delta+1<0$. At the same time, since $\tilde{y}$ should be also positive, we obtain $p>2$ which contradicts to the assumption $0\le p<-2+2\sqrt{2}$. Thus, the point (12) is not defined for $0<p<-2+2\sqrt{2}$. However, for $p>-2+2\sqrt{2}$, both coordinates become positive if $\beta-\delta+1>0$ and $p>2$. Thus we obtain the existence condition of (12) as

$$p>2,\quad \beta-\delta+1>0. \tag{16}$$

We finally investigate the existence condition of the interior fixed point P_3 (15), which naturally yields existence conditions $\beta-\delta+1>0$ and $p\ge 6(\beta-\delta)-2$ since the total sum of three species should not exceed 1. □

The stability of each fixed point can be investigated by linear stability analysis. Here, we define

$$\begin{aligned}f_1&=x\left[1-\left(1+\frac{p}{2}\right)x-y-2z+\beta-\delta\right],\\ f_2&=y\left[1-2x-\left(1+\frac{p}{2}\right)y-z+\beta-\delta\right],\\ f_3&=z\left[1-x-2y-\left(1+\frac{p}{2}\right)z+\beta-\delta\right],\end{aligned}$$

and the Jacobian matrix **J** of the equation system is

$$\mathbf{J}=\begin{bmatrix}\frac{\partial f_1(x,y,z)}{\partial x} & -x & -2x\\ -2y & \frac{\partial f_2(x,y,z)}{\partial y} & -y\\ -z & -2z & \frac{\partial f_3(x,y,z)}{\partial z}\end{bmatrix}, \tag{17}$$

where

$$\begin{aligned}\frac{\partial f_1(x,y,z)}{\partial x}&=1-(p+2)x-y-2z+(\beta-\delta),\\ \frac{\partial f_2(x,y,z)}{\partial y}&=1-2x-(p+2)y-z+(\beta-\delta),\\ \frac{\partial f_3(x,y,z)}{\partial z}&=1-x-2y-(p+2)z+(\beta-\delta).\end{aligned}$$

From the Jacobian matrix (17), we obtain associated eigenvalues for the fixed points (9)–(11) of P_1 as:

$$\begin{aligned}&\lambda_1=\delta-\beta-1,\quad \lambda_2=\frac{p(\beta-\delta+1)}{p+2},\\ &\lambda_3=\frac{(p-2)(\beta-\delta+1)}{p+2},\end{aligned} \tag{18}$$

where all points of P_1 have same eigenvalues.

Since $\beta-\delta+1>0$, we find that λ_1 in (18) is negative, and λ_2 is positive for $p\in\mathbb{R}_+$. Thus, the fixed points (9)–(11) are always unstable, but they can constitute heteroclinic cycles in which are asymptotically stable when λ_3 is negative, i.e., $p<2$. To be concrete, the heteroclinic cycle can be asymptotically stable when $p<1$ as proven in Theorem 1.

Theorem 1. *Three absorbing fixed points (9)–(11) can constitute heteroclinic cycles in which are asymptotically stable for* $p<1$ *when the points are defined.*

Proof. To identify the exact condition for the stability of the heteroclinic cycles, we need to calculate the saddle value V: [50]

$$V=\prod_{i=1}^{3}V_i=\prod_{i=1}^{3}\left(-\frac{\lambda_{s_1}}{\lambda_u}\bigg|_i\right), \tag{19}$$

where eigenvalues satisfy $\lambda_u>0>\lambda_{s_1}>\lambda_{s_2}$. Since $\beta+1>\delta$, we have

$$\begin{aligned}\lambda_3-\lambda_1&=\frac{(p-2)(\beta-\delta+1)}{p+2}-(\delta-\beta-1)\\ &=\left(\frac{p-2}{p+2}+1\right)(\beta-\delta+1)\\ &=\frac{2p}{p+2}(\beta-\delta+1)>0,\end{aligned}$$

for $p<2$, which yields $\lambda_3>\lambda_1$, and hence V_i at each point of P_1 can be calculated by

$$V_i=-\frac{\lambda_{s_1}}{\lambda_u}=-\frac{\lambda_3}{\lambda_2}$$

since $\lambda_u=\lambda_2$ which is always positive for $p>0$. According to the definition of V (19), we obtain V as a form:

$$V=\prod_{i=1}^{3}V_i=\prod_{i=1}^{3}\left(-\frac{\lambda_3}{\lambda_2}\right)=\left(-\frac{\lambda_3}{\lambda_2}\right)^3=\left(\frac{2-p}{p}\right)^3,$$

and $V>1$ for $p<1$, which implies the heteroclinic cycles are asymptotically stable. Otherwise, we obtain $V\le 1$ and thus the heteroclinic cycles are unstable (see Fig. 8). □

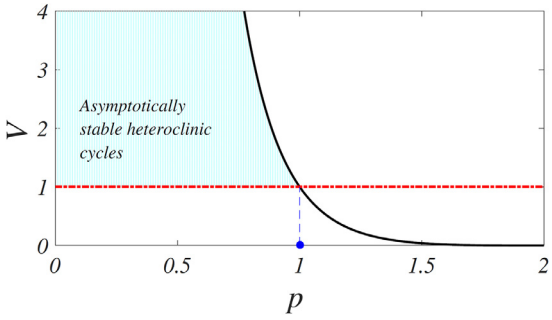

Fig. 8. The value V as a function of p.

For the fixed points (12)–(14) of P_2, corresponding eigenvalues can be found from the Jacobian argument with **J** as followings:

$$\lambda_1 = \delta - \beta - 1, \quad \lambda_2 = \frac{p(2-p)(\beta-\delta+1)}{p^2+4p-4},$$
$$\lambda_3 = \frac{(p^2-2p+4)(\beta-\delta+1)}{p^2+4p-4}, \tag{20}$$

Theorem 2. *Three fixed points (12)–(14) of P_2 are always unstable.*

Proof. According to the conditions (16), we easily find that λ_1 and λ_2 in (20) are always negative. Thus, the stability will be handled by controlling λ_3 in (20), but the λ_3 is always positive since $p^2-2p+4=(p-1)^2+3>0$ for $p>2$. Therefore, we conclude that three fixed points (12)–(14) of P_2 do not exist as stable states even if the points are well-defined. □

The linear stability with **J** yields eigenvalues associated to the interior fixed point (15) as

$$\lambda_1 = \delta - \beta - 1, \quad \lambda_{2,3} = \frac{(\beta-\delta+1)(1-p\pm\sqrt{3}i)}{p+8}, \tag{21}$$

where real and imaginary parts of $\lambda_{2,3}$ are identified by:

$$Re(\lambda_{2,3}) = \frac{(1-p)(\beta-\delta+1)}{p+8},$$
$$Im(\lambda_{2,3}) = \frac{\sqrt{3}(\beta-\delta+1)}{p+8}. \tag{22}$$

From the condition $\beta+1>\delta$ in Proposition 1, it is obvious that λ_1 is always negative. Since $\lambda_{2,3}$ are complex eigenvalues, the stability of the interior fixed point (15) ultimately depends on the sign of $Re(\lambda_{2,3})$. Since $\beta+1>\delta$, we easily find that $Re(\lambda_{2,3})<0$ if $p>1$, and thus the point (15) is asymptotically stable when it is defined. Thus we obtained the following theorem.

Theorem 3. *The interior fixed point (15) of Eq. (5) is asymptotically stable for $p>1$.*

4.2. Imbalanced population flow

Likewise balanced population flow, most of stability analysis of fixed points are easily obtained by eigenvalues of Eq. (5). Thus, we briefly provide the analysis for Q_2 which is not derived under the balanced flow. Since we have several unknown parameters even if we fixed rates of outflows, we here provide analysis numerically by showing basins of parameters. To be concrete, we analyze the fixed point $(\tilde{x}^*, \tilde{y}^*, 0)$ associated with $Q_2(XY)$ with components:

$$\begin{cases} \tilde{x}^* = \dfrac{2(2\beta_1-2\beta_2-2\delta_1+2\delta_2+p(1+\beta_1-\delta_1))}{p^2+4p-4}, \\ \tilde{y}^* = \dfrac{2(2\beta_2-4\beta_1+4\delta_1-2\delta_2-2+p(1+\beta_2-\delta_2))}{p^2+4p-4}, \end{cases} \tag{23}$$

where the associated eigenvalues are

$$\lambda_1 = \frac{1}{p^2+4p-4}[12(\beta_1-\delta_1)-4(\beta_2-\delta_2)-4(\beta_3-\delta_3)$$
$$-2p(\beta_1-\delta_1)-4p(\beta_2-\delta_2)+4p(\beta_3-\delta_3)$$
$$-2p+(\beta_3-\delta_3+1)p^2+4],$$
$$\lambda_{2,3} = \frac{1}{2(p^2+4p-4)}[4(\beta_1-\delta_1)-2p(\beta_2-\delta_2+1)$$
$$-p^2(\beta_1+\beta_2-\delta_1-\delta_2+2)+4\pm\sqrt{A}], \tag{24}$$

with the quantity A:

$$A = (\beta_1-\delta_1)^2(p^4+16p^3+88p^2+64p-112)$$
$$+(\beta_2-\delta_2)^2(p^4+12p^3+52p^2+32p-64)$$
$$+2(\beta_1\delta_2+\beta_2\delta_1-\beta_1\beta_2-\delta_1\delta_2)$$
$$\times(p^4+14p^3+52p^2+72p-96)$$
$$+4(\beta_1-\delta_1)(p^3+18p^2-4p-8)$$
$$+4(\delta_2-\beta_2)(p^3+20p-16)+4(3p-2)^2.$$

Under the given parameter $(\delta_1,\delta_2,\delta_3)=(0.1,0.3,0.4)$ used in Section 3.2, the fixed point (23) can be defined by:

$$\left(\frac{20(\beta_1-\beta_2)+(10\beta_1+9)p+4}{5(p^2+4p-4)}, \frac{20(\beta_2-2\beta_1)+(10\beta_2+7)p-22}{5(p^2+4p-4)}, 0\right), \tag{25}$$

and the eigenvalues are rewritten by

$$\lambda_1 = \frac{1}{5(p^2+4p-4)} \times [20(3\beta_1-\beta_2-\beta_3)-11p$$
$$-10p(\beta_1+2\beta_2-2\beta_3)+(5\beta_3+3)p^2+28],$$
$$\lambda_{2,3} = \frac{1}{10(p^2+4p-4)} \times [10(2\beta_1-\beta_2)$$
$$-\{5(\beta_1+\beta_2)+8\}p^2-7p+18\pm\sqrt{A'}],$$

where the quantity A' is

$$A' = 25\beta_1^2(p^4+16p^3+88p^2+64p-112)$$
$$+25\beta_2^2(p^4+12p^3+52p^2+32p-64)$$
$$+10\beta_1(p^4+23p^3+214p^2+36p-168)$$
$$-50\beta_1\beta_2(p^4+14p^3+52p^2+72p-96)$$
$$-10\beta_2(p^4+21p^3+52p^2+212p-208)$$
$$+p^4+30p^3+781p^2-580p-28.$$

From the formation in (25), we find the point is defined by β_1, β_2, and p. In particular, since β_3 only affects on λ_1, we assume $\beta_3=0.5$, and the basin of parameters for the stable (25) can be depicted as Fig. 9 when it is defined.

As we explored in Section 3.2, the fixed point (25) appears when $p=1$ as stable state. However, from the basin structure in Fig. 9, we found that the point can be stable when $p=0.83$ with very narrow region. The area of the basin is expanding as p increases, which means that the stronger intragroup competition can promote the stable survival of groups X and Y. Since we restrict the level of all inflow rates, corresponding basins only appear in small regions in Fig. 4, which are indicated in Figs. 9(d)-9(h). Stability of other fixed points can be similarly obtained, and we therefore omit.

5. Conclusion

Flow mechanisms that can account inflow and outflow of an individual's movements or participant's investment can be a common feature in social sciences. In particular, for cyclic governance changes among similar companies seeking to seize the market

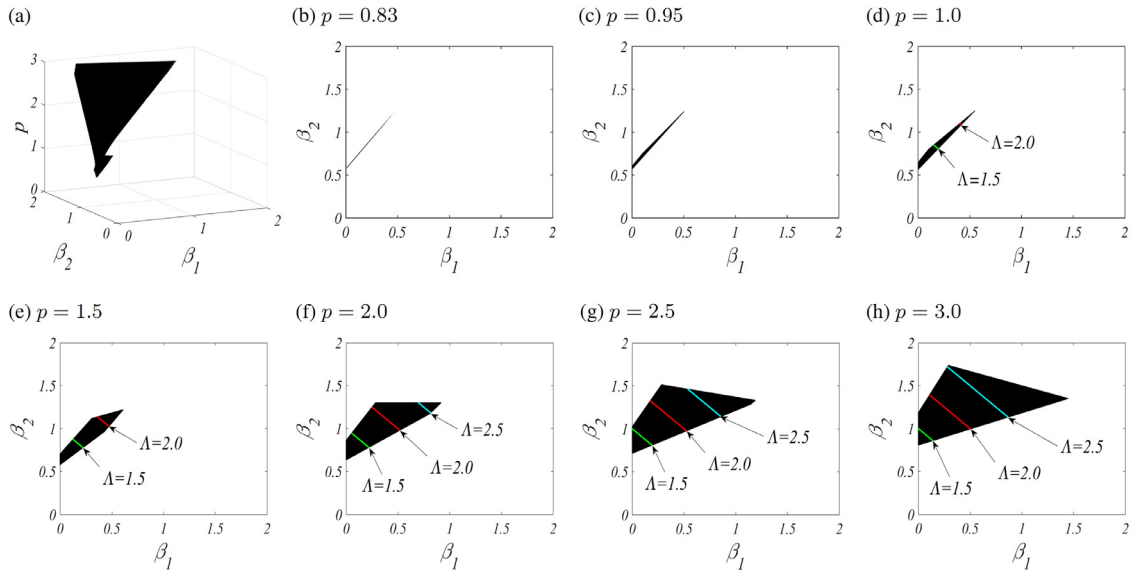

Fig. 9. Basin of parameters (β_1, β_2) for the stable (25) with different p. (a) The basin of parameters for stable (25) is presented in the three-dimensional space. (b-h) As p increases, the associated basin of (β_1, β_2) enlarges, which emerges from $p = 0.83$ with a small area. Under the restriction $\sum_{i=1}^{3} \beta_i = \Lambda$, parameters with $\beta_3 = 0.5$ associated to Fig. 4 are depicted by different colors.

through sequential launches of products and price cycling in economic markets [35,58,59], it is important to understand the flow mechanism on changes in existing commercial areas due to new commercial trends, bankruptcy or other industries. Furthermore, under the framework of ecological sciences, it is also important to understand the process of population flow as species can move in and out of society to find a better environment.

We investigated the effect of population flow on biodiversity in the system of cyclic competition which can lead the change of a community paradigm. Through numerical simulations and the linear stability analysis, we found that diversity of group survival states can be strongly promoted by population flow. If inflow and outflow rates of populations are considered as same to all groups, respectively, all groups always coexist by exhibiting a phase transition from an asymptotically stable heteroclinic cycle to a stable attractor, which corresponds to weak and strong coexistence, respectively. Such phenomena can be driven by frequent flow as the rate of intragroup competition increases. On the other hand, it has been found that the imbalanced flow where all frequencies of inflow and outflow of groups differ can yield alternative stable states. To be concrete, similar to the effect of intragroup competition [16,47], we found various survival states including the survival of any two interacting groups. We also found that the survival of the sole group can be stabilized, and the multistability among sole group survival states can emerge [31,33] which are sensitive to initial densities of groups depending on population flow. By exploiting the basin area of parameters which is measured by the number of parameters to satisfy existence and stability conditions, we have further investigated the dependency of coexistence due to relativistic interplay of population flows by changing the strength of intragroup competition, and captured oscillatory dynamics of coexistence which will provide a guideline for the robustness of coexistence behavior.

In general, the overall structure between cyclically competing groups is defined by a closed community with no population flow to the outside environment. Thus the density in a group can be only affected by one of interplay among groups, and the total density should be maintained by keeping balance among interaction interplay [15,16,47]. However, since the interplay only occurs within the same group, there is no change of a community structure even if an asymmetric system is considered. On the contrary, we suggested that population flow can be an additional candidate to destroy the symmetric structure among groups, and our suggestion can ultimately indicate the change of a community paradigm. In this regard, we expect our findings to contribute to providing global insights to interpret complex phenomena in interdisciplinary sciences.

Declaration of Competing Interest

The authors declare that they have no known competing financial interests or personal relationships that could have appeared to influence the work reported in this paper.

Acknowledgments

This research was supported by Basic Science Research Program through the National Research Foundation of Korea (NRF) funded by the Ministry of Education (No.NRF-2019R1I1A1A01043531).

Appendix A. Fixed points of Eq. (5) with imbalanced flow

Similar to the case of the balanced population flow in Section 4.1, direct calculation yields again that Eq. (5) can also possess three distinct survival states of groups which are classified by the number of surviving groups for $\beta_i, \delta_i > 0$: (a) Q_1 for existence of the only one group, (b) Q_2 for survivals of any two interacting groups, and (c) Q_3 for coexistence of all groups.

To be concrete, the Q_1 consists of three absorbing fixed points of form:

$$\left(\frac{2(\beta_1 - \delta_1 + 1)}{p+2}, 0, 0\right), \quad \left(0, \frac{2(\beta_2 - \delta_2 + 1)}{p+2}, 0\right), \quad \left(0, 0, \frac{2(\beta_3 - \delta_3 + 1)}{p+2}\right). \tag{A.1}$$

Since

$$\frac{2(\beta_i - \delta_i + 1)}{p+2} \leq 1$$

$$\Rightarrow 2(\beta_i - \delta_i + 1) \le p + 2$$
$$\Rightarrow 2(\beta_i - \delta_i) \le p,$$

each point can be defined if $2(\beta_i - \delta_i) \le p$ with $\beta_i + 1 > \delta_i$ for $p > 0$ which is similar to P_1 in Proposition 1.

For the Q_2, it also contains three fixed points of form: $(\tilde{x}^*, \tilde{y}^*, 0)$, $(0, \tilde{y}^*, \tilde{z}^*)$, and $(\tilde{x}^*, 0, \tilde{z}^*)$, where components in each case are given by

$$\begin{cases} \tilde{x}^* = \dfrac{2(2\beta_1 - 2\beta_2 - 2\delta_1 + 2\delta_2 + p(1 + \beta_1 - \delta_1))}{p^2 + 4p - 4}, \\ \tilde{y}^* = \dfrac{2(2\beta_2 - 4\beta_1 + 4\delta_1 - 2\delta_2 - 2 + p(1 + \beta_2 - \delta_2))}{p^2 + 4p - 4}. \end{cases} \tag{A.2}$$

for $(\tilde{x}^*, \tilde{y}^*, 0)$,

$$\begin{cases} \tilde{y}^* = \dfrac{2(2\beta_2 - 2\beta_3 - 2\delta_2 + 2\delta_3 + p(1 + \beta_2 - \delta_3))}{p^2 + 4p - 4}, \\ \tilde{z}^* = \dfrac{2(2\beta_3 - 4\beta_2 + 4\delta_2 - 2\delta_3 - 2 + p(1 + \beta_3 - \delta_3))}{p^2 + 4p - 4}, \end{cases} \tag{A.3}$$

for $(0, \tilde{y}^*, \tilde{z}^*)$, and

$$\begin{cases} \tilde{x}^* = \dfrac{2(2\beta_1 - 4\beta_3 - 2\delta_1 + 4\delta_3 - 2 + p(1 + \beta_1 - \delta_1))}{p^2 + 4p - 4}, \\ \tilde{z}^* = \dfrac{2(2\beta_3 - 2\beta_1 + 2\delta_1 - 2\delta_3 + p(1 + \beta_3 - \delta_3))}{p^2 + 4p - 4}, \end{cases} \tag{A.4}$$

for $(\tilde{x}^*, 0, \tilde{z}^*)$.

The Q_3, that describes the coexistence of all groups, is defined by the only one interior fixed point of the following form:

$$\frac{2(x^{**}, y^{**}, z^{**})}{p^3 + 6p^2 - 12p + 32}, \tag{A.5}$$

where the components are given by

$$\begin{aligned} x^{**} &= 12(\beta_2 - \delta_2) - 4(\beta_1 - \delta_1) - 4(\beta_3 - \delta_3) \\ &\quad + (4\beta_1 - 2\beta_2 - 4\beta_3 - 4\delta_1 + 2\delta_2 + 4\delta_3 - 2)p \\ &\quad + (\beta_1 - \delta_1 + 1)p^2 + 4, \\ y^{**} &= 12(\beta_3 - \delta_3) - 4(\beta_2 - \delta_2) - 4(\beta_1 - \delta_1) \\ &\quad + (4\beta_2 - 4\beta_1 - 2\beta_3 + 4\delta_1 - 4\delta_2 + 2\delta_3 - 2)p \\ &\quad + (\beta_2 - \delta_2 + 1)p^2 + 4, \\ z^{**} &= 12(\beta_1 - \delta_1) - 4(\beta_3 - \delta_3) - 4(\beta_2 - \delta_2) \\ &\quad + (4\beta_3 + 2\delta_1 + 4\delta_2 - 4\delta_3 - 2\beta_1 - 4\beta_2 - 2)p \\ &\quad + (\beta_3 - \delta_3 + 1)p^2 + 4. \end{aligned}$$

References

[1] Sinervo B, Lively CM. The rock-paper-scissors game and the evolution of alternative male strategies. Nature 1996;380:240–3.
[2] Jackson JCB, Buss L. Alleopathy and spatial competition among coral reef invertebrates. Proc Natl Acad Sci USA 1975;72:5160–3.
[3] Paquin CE, Adams J. Relative fitness can decrease in evolving asexual populations of S. cerevisiae. Nature 1983;306:368–71.
[4] Czárán TL, Hoekstra RF, Pagie L. Chemical warfare between microbes promotes biodiversity. Proc Natl Acad Sci USA 2002;99:786–90.
[5] Kerr B, Riley MA, Feldman MW, Bohannan BJM. Local dispersal promotes biodiversity in a real-life game of rock-paper-scissors. Nature 2002;418:171–4.
[6] Reichenbach T, Mobilia M, Frey E. Noise and correlations in a spatial population model with cyclic competition. Phys Rev Lett 2007;99:238105.
[7] Frachebourg L, Krapivsky PL, Ben-Naim E. Spatial organization in cyclic Lotka Volterra systems. Phys Rev E 1996;54:6186.
[8] Reichenbach T, Mobilia M, Frey E. Mobility promotes and jeopardizes biodiversity in rock-paper-scissors games. Nature 2007;448:1046–9.
[9] Reichenbach T, Mobilia M, Frey E. Self-organization of mobile populations in cyclic competition. J Theor Biol 2008;254:368–83.
[10] Knebel J, Krüger T, Weber MF, Frey E. Coexistence and survival in conservative Lotka Volterra networks. Phys Rev Lett 2013;110:168106.
[11] M Berr T Reichenbach MS, Frey E. Zero-one survival behavior of cyclically competing species. Phys Rev Lett 2009;102:048102.
[12] Szolnoki A, Perc M. Zealots tame oscillations in the spatial rock-paper-scissors game. Phys Rev E 2016;93:062307.
[13] Szolnoki A, Mobilia M, Jiang LL, Szczesny B, Rucklidge AM, Perc M. Cyclic dominance in evolutionary games: a review. J R Soc Interface 2014;11:20170735.
[14] Park J, Do Y, Huang Z-G, Lai Y-C. Persistent coexistence of cyclic competing species in spatially extended ecosystems. Chaos 2013;23:023128.
[15] Yang R, Wang W-X, Lai Y-C, Grebogi C. Role of intraspecific competition in the coexistence of mobile populations in spatially extended ecosystems. Chaos 2010;20:023113.
[16] Park J, Do Y, Jang B, Lai Y-C. Emergence of unusual coexistence states in cyclic game systems. Sci Rep 2017;7:7465.
[17] Mobilia M. Oscillatory dynamics in rock paper scissors games with mutations. J Theor Biol 2010;264:1–10.
[18] Toupo DFP, Strogatz SH. Nonlinear dynamics of the rock-paper-scissors game with mutations. Phys Rev E 2015;91:052907.
[19] Huang W, Haubold B, Hauert C, Traulsen A. Emergence of stable polymorphisms driven by evolutionary games between mutants. Nat Commun 2012;3:919.
[20] Szczesny B, Mobilia M, Rucklidge AM. When does cyclic dominance lead to stable spiral waves? EPL 2013;102:28012.
[21] Szczesny B, Mobilia M, Rucklidge AM. Characterization of spiraling patterns in spatial rock-paper-scissors games. Phys Rev E 2014;90:032704.
[22] Mobilia M, Rucklidge AM, Szczesny B. The influence of mobility rate on spiral waves in spatial rock-paper-scissors games. Games 2016;7:24.
[23] Yu Q, Fang D, Zhang X, Jin C, Ren Q. Stochastic evolution dynamic of the rock scissors paper game based on a quasi birth and death process. Sci Rep 2016;6:28585.
[24] Han X, Chen B, Hui C. Symmetry breaking in cyclic competition by niche construction. Appl Math Comput 2016;284:66–78.
[25] Barton AD, Dutkiewicz S, Flierl G, Bragg J, Follows MJ. Patterns of diversity in marine phytoplankton. Science 2010;327:1509–1511.
[26] Burrows S, Butler T, Jöckel P, Tost H, Kerkweg A, Pöschl U, et al. Bacteria in the global atmosphere-part 2: modeling of emissions and transport between different ecosystems. Atmos Chem Phys 2009;9:9281–97.
[27] Grošelj D, Jenko F, Frey E. How turbulence regulates biodiversity in systems with cyclic competition. Phys Rev E 2015;91:033009.
[28] Wang W-X, Ni X, Lai Y-C, Grebogi C. Pattern formation, synchronization, and outbreak of biodiversity in cyclically competing games. Phys Rev E 2011;83:011917.
[29] Park J. Emergence of oscillatory coexistence with exponentially decayed waiting times in a coupled cyclic competition system. Chaos 2019;29:071107.
[30] Ni X, Wang W-X, Lai Y-C, Grebogi C. Cyclic competition of mobile species on continuous space: pattern formation and coexistence. Phys Rev E 2010;82:066211.
[31] Park J. Multistability of extinction states in the toy model for three species. Chaos Soliton Fract 2018;114:92–8.
[32] Park J, Do Y, Jang B. Multistability in the cyclic competition system. Chaos 2018;28:113110.
[33] Park J. Changes in political party systems arising from conflict and transfer among political parties. Chaos 2018;28:061105.
[34] Wang Z, Xu B, Zhou H-J. Social cycling and conditional responses in the rock–paper-scissors game. Sci Rep 2014;4:5830.
[35] Zhou H-J. The rock paper scissors game. Contemp Phys 2016;57:151–63.
[36] Szolnoki A, Perc M, Szabó G. Defense mechanisms of empathetic players in the spatial ultimatum game. Phys Rev Lett 2012;109:078701.
[37] Szolnoki A, Perc M. Second-order free-riding on antisocial punishment restores the effectiveness of prosocial punishment. Phys Rev X 2017;7:041027.
[38] Davis K. Social sciences approaches to international migration. Popul Dev Rev 1988;14:245–61.
[39] Isserman AM. Population change and the economy: social science theories and models. Netherlands: Springer; 2012.
[40] Miles LS, Rivkin LR, Johnson MTJ, Munshi-South J, Verrelli BC. Gene flow and genetic drift in urban environments. Mol Ecol 2019;28:4138–51.
[41] Castles S. International migration at the beginning of the twenty first century: global trends and issues. Int Soc Sci J 2019;68:151–62.
[42] Mohd MH, Murray R, Plank MJ, Godsoe W. Effects of dispersal and stochasticity on the presence-absence of multiple species. Ecol Model 2016;342:49–59.
[43] Mohd MH, Murray R, Plank MJ, Godsoe W. Effects of biotic interactions and dispersal on the presence-absence of multiple species. Chaos Solitons Fractals 2017;99:185–94.
[44] Lotka AJ. Contribution to the theory of periodic reaction. J Phys Chem 1910;14:271–4.
[45] Volterra V. Variazioni e fluttuazioni del numero d'individui in specie animali conviventi.. Mem Acad Lincei Roma 1926;2:31–113.
[46] May RM, Leonard WJ. Nonlinear aspects of competition between three species. SIAM J Appl Math 1975;29:243–53.
[47] Park J. Balancedness among competitions for biodiversity in the cyclic structured three species system. Appl Math Comp 2018;320:425–36.
[48] Sneppen K, Mitarai N. Multistability with a metastable mixed state. Phys Rev Lett 2012;109:100602.
[49] Park J. Asymmetric interplay leads to robust coexistence by means of a global attractor in the spatial dynamics of cyclic competition. Chaos 2018;28:081103.
[50] Shaw KM, Park Y-M, Chiel HJ, Thomas PJ. Phase resetting in an asymptotically phaseless system: on the phase response of limit cycles verging on a heteroclinic orbit. SIAM J Appl Dyn Syst 2012;11:350–91.
[51] Bernheim BD, Whinston MD. Common agency. Econometrica 1986;54:923–42.
[52] Khalil F, Martimort D, Parigi B. Monitoring a common agent: implications for financial contracting. J Econ Theory 2007;135:35–67.

[53] Voorn B, v Genugten M, v Thiel S. Multiple principals, multiple problems: implicationsfor effective governance and a research agenda for joint service delivery. Public Adm 2019;97:671–85.
[54] Shleifer A, Vishny RW. A survey of corporate governance. J Financ 1997;52:737–83.
[55] Shi H, Wang W-X, Yang R, Lai Y-C. Basins of attraction for species extinction and coexistence in spatial rock-paper-scissors games. Phys Rev E 2010;81:030910(R).
[56] Caplat P, Anand M, Bauch C. Symmetric competition causes population oscillations in an individual-based model of forest dynamics. Ecol Model 2008;211:491–500.
[57] Mohd MH. Diversity in interaction strength promotes rich dynamical behaviours in a three-species ecological system. Appl Math Comput 2019;353:243–53.
[58] Hopkins E, Seymour RM. The stability of price dispersion under seller and consumer learning. Int Econ Rev 2002;43:1157–90.
[59] Cason TN, Friedman D, Wagener F. The dynamics of price dispersion, or Edgeworth variations. J Econ Dyn Control 2005;29:801–22.